Next generation of adeno-associated virus 2 vectors: Point mutations in tyrosines lead to high-efficiency transduction at lower doses

Li Zhong*[†‡], Baozheng Li*, Cathryn S. Mah*[†], Lakshmanan Govindasamy[†§], Mavis Agbandje-McKenna[†§], Mario Cooper*, Roland W. Herzog*[†¶], Irene Zolotukhin*, Kenneth H. Warrington, Jr.*[†], Kirsten A. Weigel-Van Aken*[†‡¶], Jacqueline A. Hobbs[‡¶‖], Sergei Zolotukhin*[†¶], Nicholas Muzyczka[†¶], and Arun Srivastava*[†‡¶]**

*Division of Cellular and Molecular Therapy, Department of Pediatrics, [†]Powell Gene Therapy Center and Genetics Institute, [‡]Shands Cancer Center, and Departments of [§]Biochemistry and Molecular Biology, [¶]Molecular Genetics and Microbiology, and [‖]Psychiatry, University of Florida College of Medicine, Gainesville, FL 32610

Communicated by Kenneth I. Berns, University of Florida College of Medicine, Gainesville, FL, March 24, 2008 (received for review February 1, 2008)

Recombinant adeno-associated virus 2 (AAV2) vectors are in use in several Phase I/II clinical trials, but relatively large vector doses are needed to achieve therapeutic benefits. Large vector doses also trigger an immune response as a significant fraction of the vectors fails to traffic efficiently to the nucleus and is targeted for degradation by the host cell proteasome machinery. We have reported that epidermal growth factor receptor protein tyrosine kinase (EGFR-PTK) signaling negatively affects transduction by AAV2 vectors by impairing nuclear transport of the vectors. We have also observed that EGFR-PTK can phosphorylate AAV2 capsids at tyrosine residues. Tyrosine-phosphorylated AAV2 vectors enter cells efficiently but fail to transduce effectively, in part because of ubiquitination of AAV capsids followed by proteasome-mediated degradation. We reasoned that mutations of the surface-exposed tyrosine residues might allow the vectors to evade phosphorylation and subsequent ubiquitination and, thus, prevent proteasome-mediated degradation. Here, we document that site-directed mutagenesis of surface-exposed tyrosine residues leads to production of vectors that transduce HeLa cells ≈10-fold more efficiently *in vitro* and murine hepatocytes nearly 30-fold more efficiently *in vivo* at a log lower vector dose. Therapeutic levels of human Factor IX (F.IX) are also produced at an ≈10-fold reduced vector dose. The increased transduction efficiency of tyrosine-mutant vectors is due to lack of capsid ubiquitination and improved intracellular trafficking to the nucleus. These studies have led to the development of AAV vectors that are capable of high-efficiency transduction at lower doses, which has important implications in their use in human gene therapy.

AAV vectors | capsid mutations | gene expression | gene therapy | gene transfer

The adeno-associated virus 2 (AAV2) is a nonpathogenic human parvovirus, which has gained attention as an alternative to the more commonly used retrovirus- and adenovirus-based vectors for gene transfer and gene therapy (1, 2). Recombinant AAV2 vectors have been shown to transduce a wide variety of cells and tissues *in vitro* and *in vivo* (2–5) and are currently in use in Phase I/II clinical trials for gene therapy of a number of diseases, such as cystic fibrosis, α-1 anti-trypsin deficiency, Parkinson's disease, Batten's disease, and muscular dystrophy (6–9). Systematic studies have been undertaken to elucidate some of the fundamental steps in the life cycle of AAV2 vectors, which include viral binding and entry (10–13), intracellular trafficking (14–18), uncoating (19, 20), second-strand DNA synthesis and transgene expression (21–27), and viral genome integration into the host cell chromosome (28–30).

The ubiquitin–proteasome pathway has been shown to play an essential role in AAV2 intracellular trafficking (17, 31, 32). In our more recent studies (33), we observed that perturbations in EGFR-PTK signaling affects AAV2 transduction efficiency by not only augmenting viral second-strand DNA synthesis but also by facilitating intracellular trafficking from the cytoplasm to the nucleus. We also reported that intact AAV2 capsids can be phosphorylated at tyrosine residues by EGFR-PTK, but not at serine/threonine residues by casein kinase II (CKII) under cell-free conditions *in vitro*, and that tyrosine-phosphorylation of AAV2 capsids negatively affects viral intracellular trafficking and transgene expression in intact cells *in vivo* (34). Based on these studies, we hypothesized that EGFR-PTK-mediated phosphorylation of capsid proteins at tyrosine residues is a prerequisite for ubiquitination of intact AAV2 particles and that a substantial number of ubiquitinated virions are recognized and degraded by cytoplasmic proteasomes on their way to the nucleus, leading to inefficient nuclear transport. We reasoned, therefore, that substitution of surface exposed tyrosine residues on AAV2 capsids might allow the vectors to escape ubiquitination and, thus, proteasome-mediated degradation.

We document here that mutations of surface-exposed tyrosine residues on AAV2 capsids circumvents the ubiquitination step, thereby avoiding proteasome-mediated degradation and resulting in high-efficiency transduction by these vectors in human cells *in vitro* and murine hepatocytes *in vivo*, leading to the production of therapeutic levels of human coagulation factor at reduced vector doses. We also observed increased transduction efficiency of tyrosine-mutant vectors due to lack of ubiquitination and improved intracellular trafficking to the nucleus. In addition to yielding insights into the role of tyrosine-phosphorylation of AAV2 capsid in various steps in the life cycle of AAV2, these studies have resulted in the development of AAV2 vectors that are capable of high-efficiency transduction at lower doses.

Results

Mutations in Surface-Exposed Tyrosine Residues Significantly Improve the Transduction Efficiency of AAV2 Vectors in HeLa Cells *in Vitro*. To test our hypothesis that tyrosine-phosphorylation of AAV2

Author contributions: L.Z., C.S.M., M.A.-M., R.W.H., S.Z., N.M., and A.S. designed research; L.Z., B.L., L.G., M.C., I.Z., and K.H.W. performed research; L.Z., C.S.M., L.G., M.A.-M., R.W.H., K.A.W.-V.A., J.A.H., S.Z., N.M., and A.S. analyzed data; and L.Z., M.A.-M., R.W.H., and A.S. wrote the paper.

Conflict of interest statement: The Sponsor declares a conflict of interest (such as defined by PNAS policy). K.I.B. is on the Scientific Advisory Board of Applied Genetic Technologies Corporation. The authors declare a conflict of interest (such as defined by PNAS policy). N.M. is an inventor of patents related to recombinant AAV technology and owns equity in a gene therapy company that is commercializing AAV for gene therapy applications.

Freely available online through the PNAS open access option.

**To whom correspondence should be addressed at: Division of Cellular and Molecular Therapy, Cancer and Genetics Research Complex, 1376 Mowry Road, Room 492-A, University of Florida College of Medicine, Gainesville, FL 32610. E-mail: aruns@peds.ufl.edu.

This article contains supporting information online at www.pnas.org/cgi/content/full/0802866105/DCSupplemental.

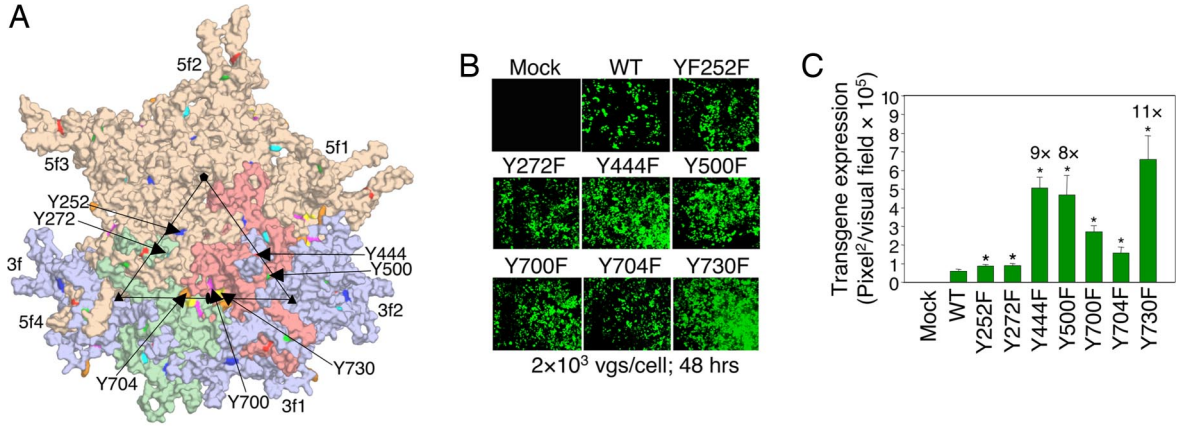

Fig. 1. Site-directed mutational analyses of surface-exposed tyrosine residues on AAV2 capsid proteins and generation of recombinant scAAV2-EGFP vectors. (*A*) A surface representation of AAV2 VP3 shown in different colors for icosahedral symmetry related monomers (salmon, reference; green, twofold; bluish purple, threefold; and wheat, fivefold). The position of the seven surface-exposed tyrosine residues on the AAV2 capsid surface, Y252, Y272, Y444, Y500, Y700, Y704, and Y730, are indicated by the arrows and colored blue, cyan, red, green, pink, orange, and yellow, respectively, on all of the VP3 monomers. The icosahedral twofold axis is shown with the filled oval, the threefold axis is shown in the red triangle, and the fivefold axis is shown in the filled pentagon. A viral asymmetric unit is shown in the open triangle. Site-directed mutations of these seven tyrosine residues to phenylalanine residues (tyrosine-phenylalanine, Y-F) were performed and tyrosine-mutant capsid scAAV2-EGFP vectors were generated. (*B*) AAV2-mediated transgene expression in HeLa cells after transduction with tyrosine-mutant capsid scAAV2-EGFP vectors. (Magnification, ×100.) (*C*) Quantitation of the transduction efficiency in HeLa cells. *, $P < 0.01$ vs. WT scAAV2-EGFP.

capsids leads to increased ubiquitination and results in impaired intracellular trafficking and is therefore unfavorable to viral transduction, we modified surface-exposed tyrosine residues on AAV2 capsids. Inspection of the capsid surface of the AAV2 structure (Fig. 1*A*), revealed a total of 7 surface-exposed tyrosine residues (Y252, Y272, Y444, Y500, Y700, Y704, and Y730). We performed site-directed mutagenesis of each of the 7 tyrosine residues, which were conservatively substituted with phenylalanine residues (tyrosine-phenylalanine, Y-F) [supporting information (SI) Table S1]. scAAV2-EGFP genomes encapsidated in each of the tyrosine-mutant capsids were successfully packaged (Table S2), and mutations of the surface-exposed tyrosine residues did not lead to reduced vector stability (data not shown).

The transduction efficiency of each of the tyrosine-mutant vectors was analyzed and compared with the WT scAAV2-EGFP vector in HeLa cells *in vitro* under identical conditions. From the results shown in Fig. 1*B*, it is evident that, although mock-infected cells showed no green fluorescence, the transduction efficiency of each of the tyrosine-mutant vectors was significantly higher compared with the WT scAAV2-EGFP vector at 2,000 viral particles per cell. Specifically, the transduction efficiency of Y444F, Y500F, and Y730F vectors was ≈8–11-fold higher than the WT vector (Fig. 1*C*).

Mutations in Surface-Exposed Tyrosine Residues Dramatically Improve the Transduction Efficiency of AAV2 Vectors in Murine Hepatocytes *in Vivo*. The efficacy of WT and tyrosine-mutant scAAV2-EGFP vectors was also evaluated in a mouse model *in vivo*. As can be seen in Fig. 2*A*, the transduction efficiency of tyrosine-mutant vectors was significantly higher and ranged from 4- to 29-fold compared with the WT vector (Fig. 2*B*). When other tissues, such as heart, lung, kidney, spleen, pancreas, GI tract (jejunum and colon), testis, skeletal muscle, and brain were harvested from mice injected with 1×10^{10} particles of the tyrosine-mutant vectors and analyzed, no evidence of EGFP gene expression was seen (data not shown). Thus, mutations in the surface-exposed tyrosine residues did not appear to alter the liver-tropism after tail vein injection of these vectors *in vivo*.

Increased Transduction Efficiency of Tyrosine-Mutant Vectors Is Due to Lack of Ubiquitination and Improved Intracellular Trafficking to the Nucleus. To further confirm our hypothesis that EGFR-PTK-mediated phosphorylation of capsid proteins at tyrosine residues is a prerequisite for ubiquitination of AAV2 capsids and that ubiquitinated virions are recognized and degraded by cytoplasmic proteasome on their way to the nucleus, leading to inefficient nuclear transport, a series of experiments were performed as follows.

In the first set of experiments, HeLa C12 cells, carrying adenovirus-inducible AAV2 *rep* and *cap* genes, were mock-infected or infected with WT, Y444F, or Y730F scAAV2-EGFP vectors. As shown in Fig. 3 *A* and *B*, whereas mock-infected cells showed no green fluorescence, and ≈15% of cells were transduced with the WT scAAV2-EGFP vectors in the absence of coinfection with adenovirus, the transduction efficiency of Y444F and Y730F scAAV2-EGFP vectors was increased by ≈9 and ≈18-fold, respectively, compared with the WT vector. Interestingly, although coinfection with adenovirus led to ≈11-fold increase in the transduction efficiency of the WT scAAV2-EGFP vectors (Fig. 3*B*), the transduction efficiency of Y444F and Y730F scAAV2-EGFP vectors was not further enhanced by coinfection with adenovirus. Because adenovirus can improve AAV2 vector nuclear transport in HeLa cells (35), these data suggest that the surface-exposed tyrosine residues play a role in intracellular trafficking of AAV2 and that their removal leads to efficient nuclear transport of AAV2 vectors.

In the second set of experiments, HeLa cells, either mock-treated or treated with Tyr-23, a specific inhibitor of EGFR-PTK (36, 37), or MG132, a proteasome inhibitor (38), both known to increase the transduction efficiency of AAV vectors, were mock-infected or infected with the WT or Y730F scAAV2-EGFP vectors. These data are shown in Fig. 3*C*. Although mock-infected cells showed no green fluorescence, and ≈5% of cells were transduced with the WT scAAV2-EGFP vectors in mock-treated cells, pretreatment with Tyr-23 or MG132 led to an ≈9-fold and ≈6-fold increase in the transduction efficiency, respectively (Fig. 3*D*). Although the transduction efficiency of Y730F scAAV2-EGFP vectors was increased by ≈14-fold compared with the WT vectors, it was not further enhanced by pretreatment with either Tyr-23 or MG132 (Fig. 3*D*). These data strongly suggest that the absence of surface-exposed tyrosine residues, which prevented phosphorylation of the mutant vectors, likely prevented ubiquitination of the capsid proteins, and these vectors on their way to the nucleus could not be recognized

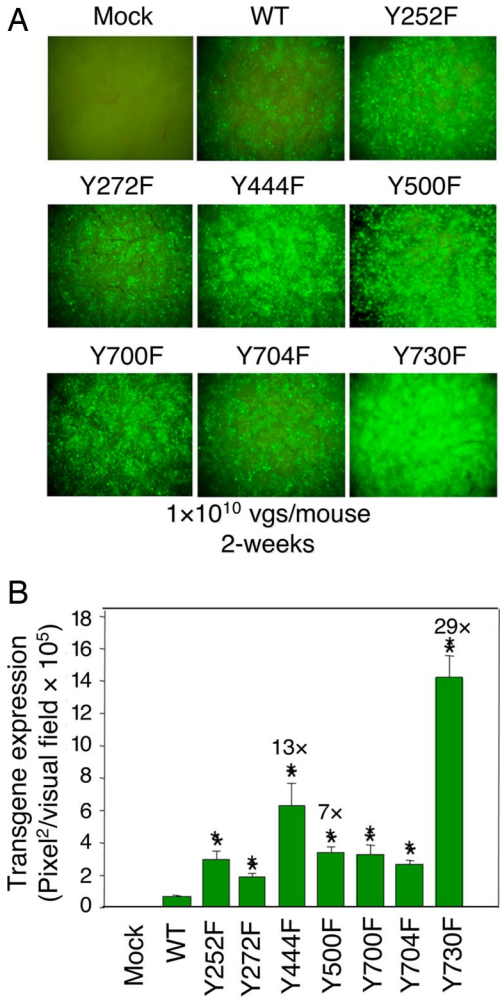

Fig. 2. AAV2-mediated transduction of hepatocytes from normal C57BL/6 mice injected via tail vein with tyrosine-mutant capsid scAAV2-EGFP vectors. (*A*) Transgene expression was detected by fluorescence microscopy 2 weeks after injection of 1×10^{10} viral particles per animal via the tail vein ($n = 2$ per experimental group). (Magnification, ×50.) (*B*) Quantitation of the transduction efficiency in hepatocytes in C57BL/6 mice. *, $P < 0.01$ vs. WT scAAV2-EGFP.

and degraded by the proteasome, which led to their efficient nuclear translocation.

In the third set of experiments, HeLa cells, either mock-treated or treated with MG132, were mock-infected or infected with the WT, Y730F, or Y444F scAAV2-EGFP vectors. Whole cell lysates (WCLs) were prepared 4 h after infection, and equivalent amounts of proteins were immunoprecipitated first with anti-AAV2 capsid antibody (A20) followed by Western blot analyses with anti-Ub monoclonal antibody. These results are shown in Fig. 4. Although ubiquitinated AAV2 capsid proteins (Ub-AAV2 Cap) were undetectable in mock-infected cells (lanes 1 and 2), the signal of ubiquitinated AAV2 capsid proteins was weaker in untreated cells (lanes 3 and 5), and a significant accumulation of ubiquitinated AAV2 capsid proteins occurred after treatment with MG132 (lane 4). Interestingly, infections with Y730F or Y444F vectors dramatically decreased the extent of accumulation of MG132-induced ubiquitinated AAV2 capsid proteins (lanes 6 and 8). These results substantiate that mutation in tyrosine residues circumvents proteasome-mediated degradation of the vectors.

In the fourth set of experiments, we examined the fate of the input WT, Y444F, and Y730F vector viral DNA in HeLa cells. Southern blot analysis of low-M_r DNA samples isolated from cytoplasmic (C) and nuclear (N) fractions (Fig. 5*A*) and densitometric scanning of autoradiographs (Fig. 5*B*) revealed that ≈36% of the input scAAV2 DNA was present in the nuclear fraction in cells infected with the WT vector (Fig. 5*A*, lane 4, and *B*), consistent with our studies in ref. 33. Interestingly, however, the amount of input Y730F and Y444F scAAV2 vector DNA in the nuclear fraction was increased to ≈72% and ≈70%, respectively (Fig. 5*B*). These results further document that mutations in the surface-exposed tyrosine residues prevent ubiquitination of AAV2 capsids, resulting in a decrease of proteasome-mediated degradation and, in turn, facilitate nuclear transport of AAV2 vectors.

Tyrosine-Mutant Vectors Express Therapeutic Levels of Human Factor IX Protein at ≈10-Fold Reduced Vector Dose in Mice. Finally, it was important to examine whether tyrosine-mutant AAV2 vectors were capable of delivering a therapeutic gene efficiently at a reduced vector dose *in vivo*. To this end, a single-stranded, hepatocyte-specific human Factor IX (hF.IX) expression cassette was encapsidated in the Y730F vector, and the efficacy of this vector was tested in three different strains of mice (BALB/c, C3H/HeJ, and C57BL/6). Consistently, in all three strains, Y730F vector achieved ≈10-fold higher circulating hF.IX levels compared with the WT vector after tail vein or portal vein administration, with the latter being the more effective route. These results, shown in Fig. 6, clearly indicate that the Y730F vectors express therapeutic levels of human F.IX protein (≈50 ng/ml) at ≈10-fold reduced vector dose (1×10^{10} particles per mouse) in C57BL/6 mice by port vein injection. It should be noted that hepatic viral gene transfer in C57BL/6 mice is generally more efficient than in the other two strains.

Discussion

More than a decade ago, we documented that specific inhibitors of cellular protein tyrosine kinases in general and EGFR-PTK in particular, but not inhibitors of cellular serine/threonine kinases, dramatically increase the transduction efficiency of ssAAV vectors (36, 37). Based on our more recent studies (33), we hypothesized that during the process of navigation through the late endosome, AAV2 capsids become phosphorylated at tyrosine residues by EGFR-PTK, which provides a putative signal for the cellular machinery to ubiquitinate the viral capsid proteins, which are subsequently targeted for degradation by the proteasome in the cytoplasm. Our hypothesis has been borne out by the data from our recent studies in that intact AAV2 capsids can indeed be phosphorylated at tyrosine residues by EGFR-PTK, but not at serine/threonine residues by CKII (34). The currently available trafficking data suggest that the acidic environment in the endosome might lead to changes in viral conformation that facilitate escape, raising the possibility that a different set of tyrosine residues than those described here may become surface exposed. However, this is not supported by our structural studies (H.-J. Nam, E.B. Miller, and M.A.-M., unpublished data).

Our data are consistent with the interpretation that EGFR-PTK-induced tyrosine phosphorylation of AAV2 capsid proteins promotes ubiquitination and degradation of AAV2, thus leading to impairment of viral nuclear transport and decrease in transduction efficiency. Mutational analyses of each of the seven surface-exposed tyrosine residues yield AAV2 vectors with significantly increased transduction efficiency *in vitro* and *in vivo*. Specifically, Y444F and Y730F mutant vectors bypass the ubiquitination step, which results in a significantly improved intracellular trafficking and delivery of the viral genome to the nucleus. Ubiquitination could be important in directing the viral particle to the nucleus through binding to ubiquitin-dependent nuclear receptors and/or in priming the vector uncoating. In addition, it is also possible that the proteasome effect may be cell type-specific (31, 39, 40).

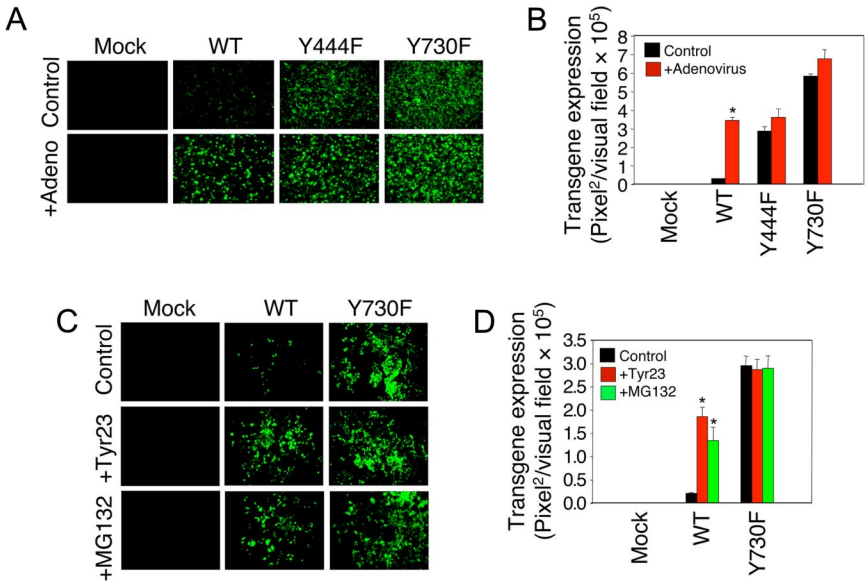

Fig. 3. Comparative analyses of AAV2-mediated transduction efficiency in HeLa C12 cells with or without coinfection with adenovirus and treatment with proteasome- or EGFR-PTK-inhibitors after transduction with tyrosine-mutant capsid scAAV2-EGFP vectors. (*A*) Cells were mock-infected or infected with adenovirus after transduction with the WT, Y444F, or Y730F scAAV2-EGFP vectors. (Magnification, 100×.) (*B*) Quantitation of the transduction efficiency in HeLa C12 cells. (*C*) Cells were mock-treated or treated with Tyr-23 or MG132, after transduction with the WT or Y730F scAAV2-EGFP vectors. (Magnification, ×100.) (*D*) Quantitation of the transduction efficiency. *, $P < 0.05$ vs. control.

Beyond providing mechanistic details of the key steps in the life cycle of AAV2, our studies have yielded an additional repertoire of AAV2-based vectors. Despite long-term therapeutic expression achieved in preclinical animal models by AAV2 vectors composed of the WT capsid proteins (41), in a recent gene therapy trial, two patients with severe hemophilia B developed vector dose-dependent transaminitis that limited duration of hepatocyte-derived hF.IX expression to <8 weeks (42). Subsequent analyses demonstrated presence of memory $CD8^+$ T cells to AAV capsids in humans and an MHC I-restricted, capsid-specific cytotoxic T lymphocyte response in one of the hemophilia B patients, which mirrored the time course of the transaminitis. It was concluded that this $CD8^+$ T cell response to input capsid eliminated AAV2-transduced hepatocytes (43). Our data show that a lower capsid antigen dose is sufficient for efficient gene transfer with the Y730F vector. It should be noted that the AAV2-F.IX vector used here contained a ssAAV genome, and we suspect that, with the use of scAAV2-F.IX Y730F mutant vector, we might be able to reduce the required vector dose further to achieve therapeutic levels of F.IX. Moreover, our data show much-reduced ubiquitination of AAV-Y730F compared with WT capsid, a prerequisite for MHC I presentation. Thus, the T cell response to AAV2 capsid, a serious hurdle for therapeutic gene transfer in the liver, might be avoidable by using the surface-exposed tyrosine-mutant AAV2 vectors. Therefore, we can likely achieve reduced MHC I presentation of capsid in target cells by two mechanisms, which should be additive in their effect.

In collaborations with our colleagues, we have also observed dramatically increased transduction efficiency of tyrosine-

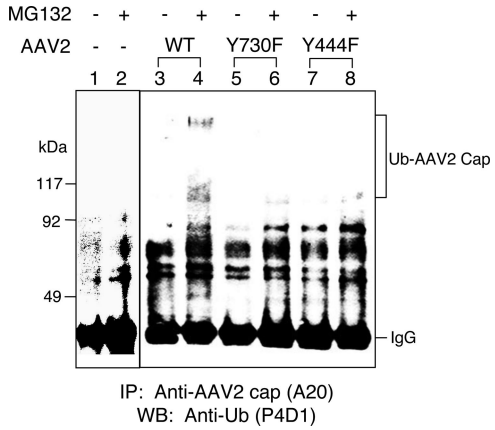

Fig. 4. Western blot analyses of ubiquitinated AAV2 capsid proteins in HeLa cells after transduction with tyrosine-mutant scAAV2-EGFP vectors. WCLs prepared from cells (untreated or treated with MG132) after mock-infection (lanes 1 and 2), or infected with the WT (lanes 3 and 4), Y730F (lanes 5 and 6), or Y444F (lanes 7 and 8) scAAV2-EGFP vectors were immunoprecipitated with anti-AAV2 capsid antibody A20 followed by Western blot analyses with anti-Ub monoclonal antibody P4D1.

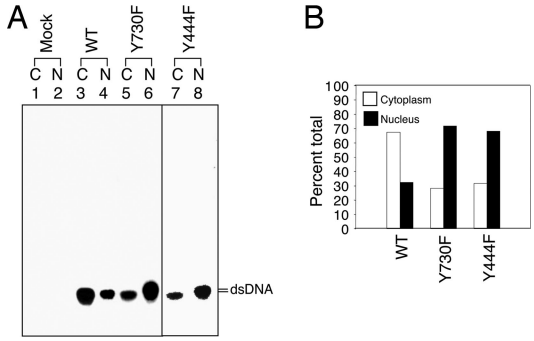

Fig. 5. Southern blot analyses of intracellular trafficking of the WT and tyrosine-mutant scAAV2-EGFP vectors and cytoplasmic (C) and nuclear (N) distribution of AAV2 genomes. HeLa cells were mock-infected (lanes 1 and 2) or infected with the WT (lanes 3 and 4), Y730F (lanes 5 and 6), or Y444F (lanes 7 and 8) scAAV2-EGFP vectors. (*A*) Nuclear and cytoplasmic fractions were obtained 18 h after infection. Low-M_r DNA samples were isolated and electrophoresed on 1% agarose gels followed by Southern blot hybridization, using a ^{32}P-labeled EGFP DNA probe. (*B*) Quantitation of relative amounts of viral genomes. These results are representative of two independent experiments.

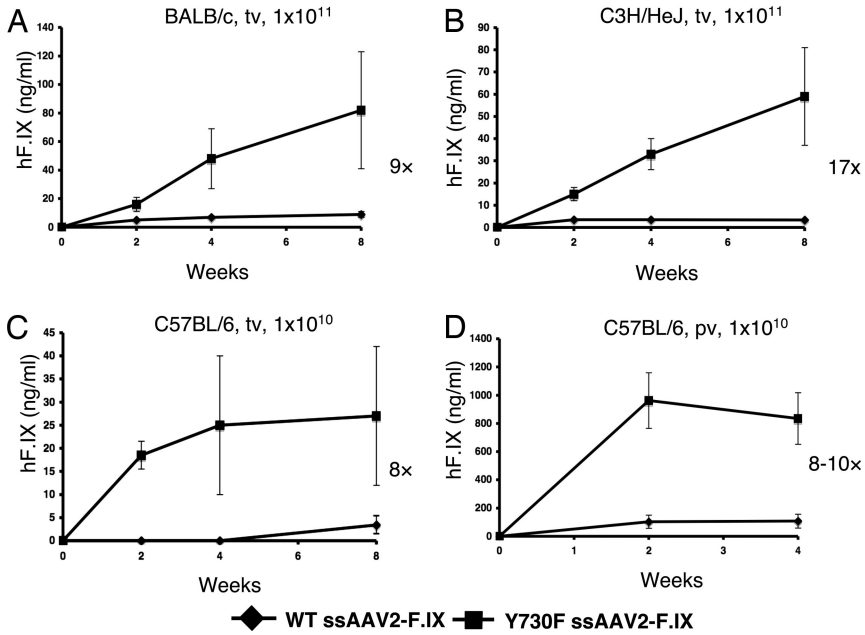

Fig. 6. Comparative analyses of the WT or Y730F ssAAV2-ApoE/hAAT-hF.IX vector-mediated transduction efficiency in hepatocytes in mice *in vivo*. Human F.IX (hF.IX) expression in plasma was determined as a function of time after injection of 1×10^{11} viral particles/animal in BALB/c (*A*), and C3H/HeJ (*B*) mice via tail vein (tv), and 1×10^{10} viral particles/animal in C57BL/6 mice via tail vein (tv) (*C*), or portal vein (pv) (*D*). Fold increase of hF.IX peak levels of Y730F vectors compared with the WT capsid vectors is indicated for each panel. Data are mean ± SD ($n = 4$ per experimental group).

mutant vectors in primary human neuronal and hematopoietic stem cells *in vitro* and in various tissues and organs in mice *in vivo* (unpublished data). We have also generated double, triple, and quadruple tyrosine-mutants to examine whether such multiple mutants are viable and whether the transduction efficiency of these vectors can be augmented further. It is noteworthy that with a few exceptions (Y444 positioned equivalent to a glycine in AAV4 and arginine in AAV5, Y700 positioned equivalent to phenylalanine in AAV4 and AAV5, and Y704 positioned equivalent to a phenylalanine in AAV7), these tyrosine residues are highly conserved in AAV serotypes 1–10, and we have also begun to generate Y-F mutants of each of these serotypes for future analyses. The availability of a vast repertoire of tyrosine-mutant AAV serotype vectors should allow us to gain a better understanding of the role of tyrosine-phosphorylation of AAV capsids in various steps in the virus life cycle, which is likely to have important implications in the optimal use of recombinant tyrosine-mutant AAV serotype vectors in human gene therapy.

Materials and Methods

Recombinant AAV2 Vectors. Highly purified stocks of scAAV2 vectors containing the enhanced green fluorescence protein (EGFP) gene driven by the chicken β-actin promoter (scAAV2-EGFP), and ssAAV2 vectors containing the human factor IX (hF.IX) gene under the control of the apolipoprotein enhancer/human α-1 antitrypsin (ApoE/hAAT) promoter (ssAAV2-hF.IX) were generated as described in ref. 44.

Localization of Surface-Tyrosines on the AAV2 Capsid Surface. The crystal structure of AAV2 (45) (PDB entry 1LP3) was used to localize the tyrosine residues on the AAV2 capsid surface. The icosahedral two-, three- and fivefold related VP3 monomers were generated by applying icosahedral symmetry operators to a reference monomer, using the program O (46) on a Silicon graphics Octane workstation. The position of the tyrosine residues were then visualized and analyzed in the context of a viral asymmetric unit, using the program COOT (47), and graphically presented by using the program PyMOL molecular graphics system (DeLano Scientific).

Construction of Surface-Exposed Tyrosine Residue Mutant AAV2 Capsid Plasmids. A two-stage procedure, based on QuikChange II site-directed mutagenesis (Stratagene) was performed by using plasmid pACG-2 as described in ref. 48. Briefly, in stage one, two PCR extension reactions were performed in separate tubes for each mutant. One tube contained the forward PCR primer and the other contained the reverse primer (Table S1). In stage two, the two reactions were mixed and a standard PCR mutagenesis assay was carried out as per the manufacturer's instructions. PCR primers were designed to introduce changes from tyrosine to phenylalanine residues and a silent change to create a new restriction endonuclease site for screening purposes (Table S1). All mutants were screened with the appropriate restriction enzyme and were sequenced before use.

Preparation of WCLs and Coimmunoprecipitations. WCLs were prepared as described in refs. 18, 24, and 49. Approximately 2×10^6 HeLa cells, mock-treated or treated with MG132, were also subjected to mock-infection or infection with the WT scAAV2-EGFP, Y730F, or Y444F mutant vectors at 5×10^3 particles per cell for 2 h at 37°C. For immunoprecipitations, cells were treated with 0.01% trypsin and washed extensively with PBS. WCLs were cleared of nonspecific binding by incubation with 0.25 mg of normal mouse IgG together with 20 μl of protein G-agarose beads. After preclearing, 2 μg of capsid antibody against intact AAV2 particles (mouse monoclonal IgG_3, clone A20; Research Diagnostics), or 2 μg of normal mouse IgG (as a negative control) were added and incubated at 4°C for 1 h, followed by precipitation with protein G-agarose beads. Western blot analyses were performed as described in refs. 18, 24, and 49. For immunoprecipitations, resuspended pellet solutions were used for SDS/PAGE. Membranes were treated with monoclonal HRP-conjugated anti-Ub antibody (1:2,000 dilution) specific for ubiquitin (Ub) (mouse monoclonal IgG_1 [IgG_1], clone P4D1; Santa Cruz Biotechnology). Immuno-reactive bands were visualized by using chemiluminescence (ECL-Plus; Amersham Pharmacia Biotech).

Isolation of Nuclear and Cytoplasmic Fractions from HeLa Cells. Nuclear and cytoplasmic fractions from HeLa cells were isolated as described in refs. 14, 20, and 33. Mock-infected or recombinant WT scAAV2-EGFP, Y730F, or V444F vector-infected cells were used to isolate the cytoplasmic and nuclear fractions. The purity of each fraction was determined to be >95%, as described in ref. 14.

Southern Blot Analysis for AAV2 Trafficking. Low-M_r DNA samples from nuclear and cytoplasmic fractions were isolated and electrophoresed on 1% agarose gels or 1% alkaline-agarose gels followed by Southern blot hybridization, using a ^{32}P-labeled EGFP-specific DNA probe as described in refs. 14, 20, and 33.

Recombinant AAV2 Vector Transduction Assays *in Vitro*. Approximately 1×10^5 HeLa cells were used for transductions with recombinant AAV2 vectors as described in ref. 33. The transduction efficiency was measured 48 h after

transduction by EGFP imaging, using fluorescence microscopy. Images from three to five visual fields were analyzed quantitatively by ImageJ analysis software (National Institutes of Health, Bethesda, MD). Transgene expression was assessed as total area of green fluorescence (pixels squared) per visual field (mean ± SD). ANOVA was used to compare between test results and the control and they were determined to be statistically significant.

Recombinant AAV2 Vector Transduction Studies *in Vivo*. scAAV2-EGFP vectors were injected intravenously via the tail vein into C57BL/6 mice at 1×10^{10} virus particles per animal. Liver sections from three hepatic lobes of the mock-injected and injected mice 2 weeks after injection were mounted on slides. The transduction efficiency was measured by EGFP imaging as described above. ssAAV2-hF.IX vectors were injected intravenously (via the tail vein) or into the portal vein of C57BL/6, BALB/c, and C3H/HeJ mice at 1×10^{10} or 1×10^{11} virus particles per animal. Plasma samples were obtained by retro-orbital bleed and analyzed for hF.IX expression by ELISA as described in ref. 50.

ACKNOWLEDGMENTS. We thank Drs. Philip R. Johnson, R. Jude Samulski, and Xiao Xiao for their kind gifts of the cell line and plasmids, respectively, and K.I.B. and Dr. Dennis Steindler for a critical review of this manuscript. The Powell Gene Therapy Center Vector Core assisted with the recombinant AAV vector production, and the Pathology Core assisted with transgene expression analyses. This work was supported in part by Roche Foundation for Anemia Research Grant 8187368876 (to L.Z.), American Heart Association Scientist Development Grant (to C.S.M.), and National Institutes of Health Public Health Service Grants R01 GM-082946 and P01 HL-51811 (to M.A.-M. and S.Z.); R01 GM-082946 and P01 HL-51811 (to M.A.-M., N.M., and S.Z.), R01 DK-062302 (to S.Z.); P01 HL-078810-Project 3 (to R.W.H.); and R01 EB-002073, R01 HL-65570, R01 HL-07691, and P01 DK 058327-Project 1 (to A.S.).

1. Berns KI, Giraud C (1996) Biology of adeno-associated virus. *Curr Top Microbiol Immunol* 218:1–23.
2. Muzyczka N (1992) Use of adeno-associated virus as a general transduction vector for mammalian cells. *Curr Top Microbiol Immunol* 158:97–129.
3. Flotte TR, *et al.* (1993) Stable *in vivo* expression of the cystic fibrosis transmembrane conductance regulator with an adeno-associated virus vector. *Proc Natl Acad Sci USA* 90:10613–10617.
4. Snyder RO, *et al.* (1997) Persistent and therapeutic concentrations of human factor IX in mice after hepatic gene transfer of recombinant AAV vectors. *Nat Genet* 16:270–276.
5. Xiao X, Li J, Samulski RJ (1996) Efficient long-term gene transfer into muscle tissue of immunocompetent mice by adeno-associated virus vector. *J Virol* 70:8098–8108.
6. Flotte T, *et al.* (1996) A phase I study of an adeno-associated virus-CFTR gene vector in adult CF patients with mild lung disease. *Hum Gene Ther* 7:1145–1159.
7. Kay MA, *et al.* (2000) Evidence for gene transfer and expression of factor IX in haemophilia B patients treated with an AAV vector. *Nat Genet* 24:257–261.
8. Flotte TR, *et al.* (2004) Phase I trial of intramuscular injection of a recombinant adeno-associated virus alpha 1-antitrypsin (rAAV2-CB-hAAT) gene vector to AAT-deficient adults. *Hum Gene Ther* 15:93–128.
9. Snyder RO, Francis J (2005) Adeno-associated viral vectors for clinical gene transfer studies. *Curr Gene Ther* 5:311–321.
10. Summerford C, Samulski RJ (1998) Membrane-associated heparan sulfate proteoglycan is a receptor for adeno-associated virus type 2 virions. *J Virol* 72:1438–1445.
11. Qing K, *et al.* (1999) Human fibroblast growth factor receptor 1 is a co-receptor for infection by adeno-associated virus 2. *Nat Med* 5:71–77.
12. Summerford C, Bartlett JS, Samulski RJ (1999) AlphaVbeta5 integrin: A co-receptor for adeno-associated virus type 2 infection. *Nat Med* 5:78–82.
13. Kashiwakura Y, *et al.* (2005) Hepatocyte growth factor receptor is a coreceptor for adeno-associated virus type 2 infection. *J Virol* 79:609–614.
14. Hansen J, Qing K, Kwon HJ, Mah C, Srivastava A (2000) Impaired intracellular trafficking of adeno-associated virus type 2 vectors limits efficient transduction of murine fibroblasts. *J Virol* 74:992–996.
15. Hansen J, Qing K, Srivastava A (2001) Adeno-associated virus type 2-mediated gene transfer: Altered endocytic processing enhances transduction efficiency in murine fibroblasts. *J Virol* 75:4080–4090.
16. Sanlioglu S, *et al.* (2000) Endocytosis and nuclear trafficking of adeno-associated virus type 2 are controlled by rac1 and phosphatidylinositol-3 kinase activation. *J Virol* 74:9184–9196.
17. Douar AM, Poulard K, Stockholm D, Danos O (2001) Intracellular trafficking of adeno-associated virus vectors: Routing to the late endosomal compartment and proteasome degradation. *J Virol* 75:1824–1833.
18. Zhao W, *et al.* (2006) Role of cellular FKBP52 protein in intracellular trafficking of recombinant adeno-associated virus 2 vectors. *Virology* 353:283–293.
19. Thomas CE, Storm TA, Huang Z, Kay MA (2004) Rapid uncoating of vector genomes is the key to efficient liver transduction with pseudotyped adeno-associated virus vectors. *J Virol* 78:3110–3122.
20. Zhong L, *et al.* (2004) Impaired nuclear transport and uncoating limit recombinant adeno-associated virus 2 vector-mediated transduction of primary murine hematopoietic cells. *Hum Gene Ther* 15:1207–1218.
21. Ferrari FK, Samulski T, Shenk T, Samulski RJ (1996) Second-strand synthesis is a rate-limiting step for efficient transduction by recombinant adeno-associated virus vectors. *J Virol* 70:3227–3234.
22. Fisher KJ, *et al.* (1996) Transduction with recombinant adeno-associated virus for gene therapy is limited by leading-strand synthesis. *J Virol* 70:520–532.
23. Qing K, *et al.* (2001) Adeno-associated virus type 2-mediated gene transfer: Role of cellular FKBP52 protein in transgene expression. *J Virol* 75:8968–8976.
24. Zhong L, *et al.* (2004) Heat-shock treatment-mediated increase in transduction by recombinant adeno-associated virus 2 vectors is independent of the cellular heat-shock protein 90. *J Biol Chem* 279:12714–12723.
25. Zhong L, *et al.* (2004) Improved transduction of primary murine hepatocytes by recombinant adeno-associated virus 2 vectors *in vivo*. *Gene Ther* 11:1165–1169.
26. Zhong L, *et al.* (2004) Self-complementary adeno-associated virus 2 (AAV)-T cell protein tyrosine phosphatase vectors as helper viruses to improve transduction efficiency of conventional single-stranded AAV vectors *in vitro* and *in vivo*. *Mol Ther* 10:950–957.
27. Zhong L, *et al.* (2008) Single-polarity recombinant adeno-associated virus 2 vector-mediated transgene expression *in vitro* and *in vivo*: mechanism of transduction. *Mol Ther* 16:290–295.
28. Tan M, Qing K, Zhou S, Yoder MC, Srivastava A (2001) Adeno-associated virus 2-mediated transduction and erythroid lineage-restricted long-term expression of the human beta-globin gene in hematopoietic cells from homozygous beta-thalassemic mice. *Mol Ther* 3:940–946.
29. Zhong L, *et al.* (2006) Evaluation of primitive murine hematopoietic stem and progenitor cell transduction *in vitro* and *in vivo* by recombinant adeno-associated virus vector serotypes 1 through 5. *Hum Gene Ther* 17:321–333.
30. McCarty DM, Young SM, Jr, Samulski RJ (2004) Integration of adeno-associated virus (AAV) and recombinant AAV vectors. *Annu Rev Genet* 38:819–845.
31. Duan D, Yue Y, Yan Z, Yang J, Engelhardt JF (2000) Endosomal processing limits gene transfer to polarized airway epithelia by adeno-associated virus. *J Clin Invest* 105:1573–1587.
32. Ding W, Zhang LN, Yeaman C, Engelhardt JF (2006) rAAV2 traffics through both the late and the recycling endosomes in a dose-dependent fashion. *Mol Ther* 13:671–682.
33. Zhong L, *et al.* (2007) A dual role of EGFR protein tyrosine kinase signaling in ubiquitination of AAV2 capsids and viral second-strand DNA synthesis. *Mol Ther* 15:1323–1330.
34. Zhong L, *et al.* (2007) Tyrosine-phosphorylation of AAV2 capsid proteins and its consequences on viral intracellular trafficking and transgene expression. *Mol Ther* 15S:149.
35. Xiao W, Warrington KH, Jr, Hearing P, Hughes J, Muzyczka N (2002) Adenovirus-facilitated nuclear translocation of adeno-associated virus type 2. *J Virol* 76:11505–11517.
36. Qing K, *et al.* (1997) Role of tyrosine phosphorylation of a cellular protein in adeno-associated virus 2-mediated transgene expression. *Proc Natl Acad Sci USA* 94:10879–10884.
37. Mah C, *et al.* (1998) Adeno-associated virus type 2-mediated gene transfer: Role of epidermal growth factor receptor protein tyrosine kinase in transgene expression. *J Virol* 72:9835–9843.
38. Yan Z *et al.* (2002) Ubiquitination of both adeno-associated virus type 2 and 5 capsid proteins affects the transduction efficiency of recombinant vectors. *J Virol* 76:2043–2053.
39. Pajusola K, *et al.* (2002) Cell-type-specific characteristics modulate the transduction efficiency of adeno-associated virus type 2 and restrain infection of endothelial cells. *J Virol* 76:11530–11540.
40. Yan Z, *et al.* (2004) Distinct classes of proteasome-modulating agents cooperatively augment recombinant adeno-associated virus type 2 and type 5-mediated transduction from the apical surfaces of human airway epithelia. *J Virol* 78:2863–2874.
41. Warrington KH, Jr, Herzog RW (2006) Treatment of human disease by adeno-associated viral gene transfer. *Hum Genet* 119:571–603.
42. Manno CS, *et al.* (2006) Successful transduction of liver in hemophilia by AAV-Factor IX and limitations imposed by the host immune response. *Nat Med* 12:342–347.
43. Mingozzi F, *et al.* (2007) CD8(+) T cell responses to adeno-associated virus capsid in humans. *Nat Med* 13:419–422.
44. Auricchio A, Hildinger M, O'Connor E, Gao GP, Wilson JM (2001) Isolation of highly infectious and pure adeno-associated virus type 2 vectors with a single-step gravity-flow column. *Hum Gene Ther* 12:71–76.
45. Xie Q, *et al.* (2002) The atomic structure of adeno-associated virus (AAV-2), a vector for human gene therapy. *Proc Natl Acad Sci USA* 99:10405–10410.
46. Jones TA, Zou JY, Cowan SW, Kjeldgaard M (1991) Improved methods for building protein models in electron density maps and the location of errors in these models. *Acta Crystallogr A* 47 (Pt 2):110–119.
47. Emsley P, Cowtan K (2004) COOT: Model-building tools for molecular graphics. *Acta Crystallogr D Biol Crystallogr* 60:2126–2132.
48. Wang W, Malcolm BA (1999) Two-stage PCR protocol allowing introduction of multiple mutations, deletions and insertions using QuikChange site-directed mutagenesis. *Biotechniques* 26:680–682.
49. Zhong L, Su JY (2002) Isoflurane activates PKC and Ca^{2+}-calmodulin-dependent protein kinase II via MAP kinase signaling in cultured vascular smooth muscle cells. *Anesthesiology* 96:148–154.
50. Mingozzi F, *et al.* (2003) Induction of immune tolerance to coagulation factor IX antigen by *in vivo* hepatic gene transfer. *J Clin Invest* 111:1347–1356.